A ratiometric fluorescent quantum dots based biosensor for organophosphorus pesticides detection by inner-filter effect

Xu Yan, Hongxia Li, Xiaosong Han, Xingguang Su

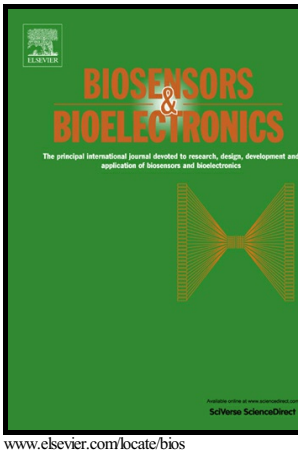

www.elsevier.com/locate/bios

PII: S0956-5663(15)30185-8
DOI: http://dx.doi.org/10.1016/j.bios.2015.06.020
Reference: BIOS7756

To appear in: *Biosensors and Bioelectronic*

Received date: 24 March 2015
Revised date: 26 May 2015
Accepted date: 9 June 2015

Cite this article as: Xu Yan, Hongxia Li, Xiaosong Han and Xingguang Su, A ratiometric fluorescent quantum dots based biosensor for organophosphoru pesticides detection by inner-filter effect, *Biosensors and Bioelectronic* http://dx.doi.org/10.1016/j.bios.2015.06.020

A ratiometric fluorescent quantum dots based biosensor for organophosphorus pesticides detection by inner-filter effect

Xu Yan[a], Hongxia Li[b], Xiaosong Han[c,d], and Xingguang Su[a,*]

[a] *Department of Analytical Chemistry, College of Chemistry, Jilin University, Changchun, 130012, China*

[b] *School of Pharmacy, Jilin University, Changchun 130021, China*

[c] *College of Computer Science and Technology, Jilin University, Changchun, 130012, China*

[d] *Talent Development Institute, Daqing Oilfield Company, CNPC, 163000, China*

*Corresponding author

Tel.: +86-431-85168352

E-mail address: *suxg@jlu.edu.cn*

Abstract

In this work, we develop a novel and sensitive sensor for the detection of organophosphorus pesticides based on the inner-filter effect (IFE) between gold nanoparticles (AuNPs) and ratiometric fluorescent quantum dots (RF-QDs). The RF-QDs has been designed by hybridizing two differently colored CdTe QDs, in which the red emissive QDs entrapped in the silica sphere acting as the reference signal, and the green emissive QDs covalently attached on the silica surface serving as the response signal. The fluorescence of RF-QDs could be quenched by AuNPs based on IFE. Protamine could effectively turn on the fluorescence due to the electrostatic attraction between protamine and AuNPs. Trypsin can easily hydrolyze protamine, leading to the quench of the fluorescence. Then, the fluorescence could be recovered again by the addition of parathion-methyl (PM) which could inhibit the activity of trypsin. By measuring the fluorescence of RF-QDs, the inhibition efficiency of PM to trypsin activity was evaluated. Under the optimized conditions, the inhibition efficiency was proportional to the logarithm of PM concentration in the range of 0.04 to 400 ng mL^{-1}, with a detection limit of 0.018 ng mL^{-1}. Furthermore, the simple and convenient method had been used for PM detection in environmental and agricultural samples with satisfactory results.

Key words: Ratiometric fluorescent quantum dots; Gold nanoparticle; Organophosphorus pesticides; Inner-filter effect

1. Introduction

Ratiometric fluorescent methods, which detect the analyte by measuring the change of the ratios of photoluminescence (PL) intensities at two wavelengths, have received intense attention in recent years (Wu et al., 2012; Chen et al., 2013; Tyrakowski et al., 2014; Yan et al., 2014a). Ratiometric fluorescence technique can provide built-in correction that eliminates false signals emanating from environmental effects and thus possess advantages in terms of improved sensitivity and accuracy (Wang et al., 2015). Till now, most ratiometric sensors employing fluorescent organic dyes are susceptible to photobleaching, low fluorescence quantum yield, exhibit generally broad emission bands and narrow excitation wavelength range, and especially the complexity of organic molecular synthesis and purification (Zong et al., 2011; Wu et al., 2013; Yao et al., 2013). Compared with those ratiometric sensors, ratiometric fluorescent-quantum dots (RF-QDs) show several advantages, such as better stability with respect to photobleaching, narrower spectral line-width and easier preparation (Zhang et al., 2011; Yao et al., 2013; Wang et al., 2015). More importantly, RF-QDs are simply obtained by combining two differently colored QDs in one nanoparticle, one kind of QDs as reference and another as a signal report unit. Thus, RF-QDs could be employed as powerful tools in chemical and biological sensing application.

Organophosphorus pesticides (OPs) have been widely used in agriculture due to their high effectiveness for controlling sucking and chewing insects, which comes to ensure the high production of crops and vegetables (Zhang et al., 2010; Zheng et al., 2011a, 2011b; Liu et al., 2012). Due to the widespread use of OPs, their residues have been frequently found in soil, atmosphere, groundwater, as well as agricultural products (Gao et al., 2012; Yan et al., 2015a). Unfortunately, the OPs residues could cause serious health problem for human even at very low

concentrations (Meng et al., 2013). The high toxicity of OPs is ascribed to their ability to irreversibly inhibit the activity of acetylcholinesterase and thus disrupts the mammal nervous system (Liu et al., 2012; Yi et al., 2013). Thus, it has important significance to develop a highly sensitive and reliable assay for monitoring pesticide residues to improve food safety and to protect the ecosystem.

In the past decade, great effort has been made to develop various methods to determine OPs, including the Association of Official Analytical Chemists methods (Huang et al., 2002; Zacharis et al., 2012), electrochemical analysis (Jha et al., 2010; Du et al., 2011; Zhang et al., 2012; Liu et al., 2014), and enzyme-linked immunosorbent assays (Yan et al., 2014b). Although these methods mentioned above have high selectivity and sensitivity, many of them required laborious synthetic procedures, tedious preparation and purification of samples, time-consume immobilizing processes, and sophisticated instrumentation etc., which limit their wide applications (Long et al., 2015). In order to circumvent these problems, OPs biosensors based on enzymes and QDs have been reported. The application of enzymes, such as acetylcholinesterase, organophosphorus hydrolase and tyrosinase, has attracted increasing attention and has been intensively investigated for their ability to detect OPs. For example, bi-enzymes of acetylcholinesterase and choline oxidase combined with QDs are used as biosensor to analyze OPs (Gao et al., 2012; Meng et al., 2013; Yi et al., 2013). Yan et al. developed a sensitive fluorescence probe for OPs detection by using organophosphorus hydrolase (Yan et al., 2015b). Hou et al. reported a sensitive fluorescent sensor for OPs based on L-tyrosine methyl ester functionalized carbon dots and tyrosinase (Hou et al., 2015).

In this study, we designed a new optical biosensor by means of an assembly of RF-QDs and

AuNPs for the detection of OPs. The detection strategy is shown in **Scheme 1**. An efficient inner-filter effect (IFE) would occur between RF-QDs and AuNPs, with RF-QDs acting as the donors and AuNPs as the acceptors. So the PL intensity at 540 nm of RF-QDs can be significantly quenched by AuNPs. Protamine (PRO), a cationic protein, could effectively bind to AuNPs due to the electrostatic attraction, which caused the aggregation of AuNPs (Jena et al., 2008) and resulted in the PL intensity at 540 nm of RF-QDs recover accordingly. Trypsin (TRY), which could cleave exclusively C-terminal to arginine and lysine residues, can easily hydrolyze PRO (Chen et al., 2013; Zhou et al., 2014), resulting in the de-aggregation of AuNPs and leading to the quench of the fluorescence. In the presence of OPs, the activity of TRY is inhibited by pesticides (Quistad et al., 2000; Ruark et al., 2011), which prevents the hydrolyzation of PRO, thus the fluorescence of RF-QDs is recovered again. To the best of our knowledge, the enzyme biosensor based on RF-QDs and AuNPs for pesticide detection has not been reported before.

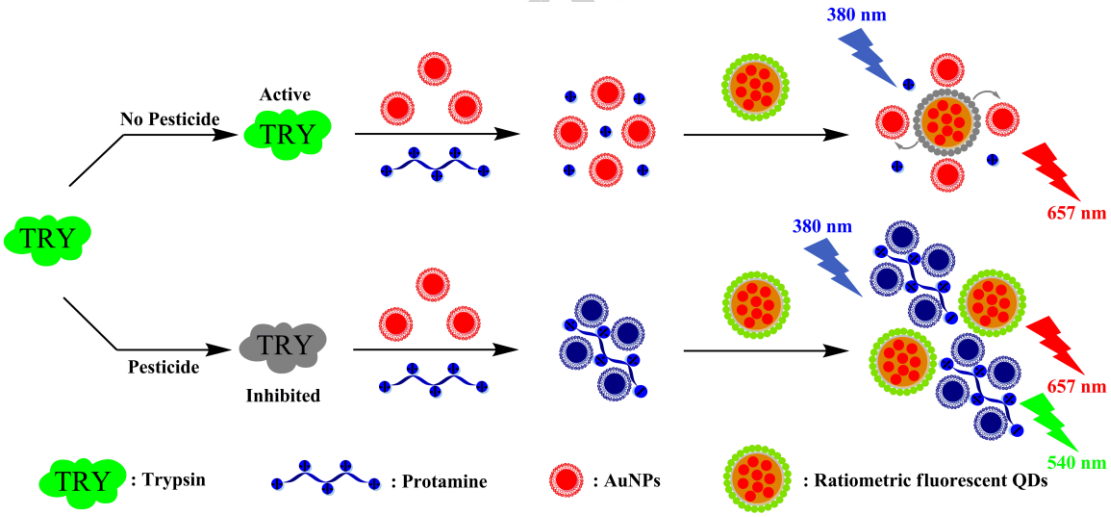

Scheme 1 Illustration of the fluorescent detection of OPs through the inner-filter effect of gold nanoparticles on RF-QDs.

2. Experiment

2.1. Reagents and instruments

All reagents and solvents were at least analytical grade and used directly without further purification. The water used in all experiments had a resistivity greater than 18 MΩ cm^{-1}. 3-Mercaptopropionic acid (MPA) (99%) was purchased from J&K Chemical Co. and tellurium powder (~200 mesh, 99.8%), $CdCl_2$ (99%) and $NaBH_4$ (99%) were purchased from Aldrich Chemical Co. Hydrogen tetrachloroaurate (III) hydrate ($HAuCl_4 \bullet xH_2O$) were purchased from Acros Organics Co., Ltd. Protamine sulfate, trypsin (1 : 250) and cetrimonium bromide (CTAB) were obtained from Beijing Dingguo Changsheng Biotechnology Company. Tetraethoxysilane (TEOS), 3-aminopropyltriethoxysilane (APTS), 1-ethyl-3-[3-dimethylaminopropyl] carbodiimide hydrochloride (EDC), N-hydroxysuccinimide (NHS), and parathion-methyl (PM) were purchased from Sigma-Aldrich Corporation.

The fluorescence spectra were obtained by using a RF-5301 PC spectrofluorophotometer (Shimadzu, Japan) equipped with a xenon lamp using right-angle geometry. Ultraviolet spectra were obtained on a Shimadzu UV-1700 UV-Visible spectrophotometer (Shimadzu Co., Kyoto, Japan). All pH measurements were made with a PHS-3C pH meter (Tuopu Co., Hangzhou, China). In both experiments, a 1 cm path-length quartz cuvette was used.

2.2. Synthesis of CdTe QDs

Water compatible CdTe QDs used in this study were synthesized by refluxing routes with mercaptopropionic acid (MPA) as stabilizer (Wang et al., 2008). Briefly, sodium hydrogen telluride (NaHTe) was produced in an aqueous solution by the reaction of sodium borohydride ($NaBH_4$) with tellurium powder at a molar ratio of 2:1. Later, NaHTe solution was added to 1.25 mmol L^{-1} $CdCl_2$ solutions at pH 11.2 in the presence of MPA with N_2 protection, and the molar

ratio of Cd^{2+}/MPA/HTe^{-} was fixed at 1:1.5:0.2. The CdTe precursor solution was subjected to a reflux at 250 °C under open-air conditions with condenser attached. Stable water-compatible MPA-capped CdTe QDs with fluorescence emission wavelength at 536 nm and 654 nm were obtained and used in the following experiments. The concentration of CdTe QDs solution is 1.23×10^{-6} mol L^{-1} (λem = 536 nm) and 9.07×10^{-6} mol L^{-1} (λem = 654 nm), respectively.

2.3. Preparation of QD@silica nanobeads and surface modification

The QD@silica nanoparticles were synthesized by the Stöber method (Yan et al., 2014a). 10 mL CTAB (1%, m/m) and 2.0 mL red emissive QDs (λem = 661 nm) were mixed and dispersed ultrasonically. Then the as-prepared solution was added to the solution with 1.0 mL water and 50 mL ethanol under vigorous stirring. Subsequently, 1.7 mL ammonium hydroxide (NH_4OH) and 200 μL TEOS were added into the reaction system and kept stirring for 15 h at room temperature. After the reaction, the prepared microspheres were washed with ethanol and water for several times to remove the unreacted chemicals. Then, the QDs@silica microspheres were dispersed in 50 mL ethanol under vigorous stirring. 100 μL APTS was introduced into the above mixture to modify the silica surface with amino groups. After 8 h of reaction, the resulting silica nanoparticles were obtained by centrifuging and washed with ethanol and ultrapure water for several times to remove the unreacted chemicals. Ultimately, the amino-modified QD@silica nanoparticles were redispersed in 10 mL of ultrapure water and preserved for further experiments.

2.4. Preparation of ratiometric fluorescent QDs (RF-QDs) nanoparticles

1.0 mL green-emitting QDs solution was dispersed in 2 mL H_2O in the flask. 2.0 mL EDC/NHS (2 mg/mL) was added, and the solution was stirred for 15 min. 3.0 mL amino-modified QD@silica nanoparticles were introduced, and the mixture was stirred for 4 h in the dark. The resulting

dual-emission silica nanoparticles were centrifuged and washed with ultrapure water for three times. The volume ratio of green QDs : red QDs=1:0.6 was used to produce the RF-QDs. The final product RF-QDs was dispersed in 10 mL ultrapure water for further use, the mass concentration of RF-QDs was 10 mg mL^{-1}.

2.5. Synthesis of gold nanoparticles (AuNPs)

13 nm AuNPs were synthesized by the reduction of $HAuCl_4$ with sodium citrate following a literature procedure (Grabar et al., 1997). Briefly, 50 mL $HAuCl_4$ (1mmol L^{-1}) was heated to reflux while stirring and then 5.0 mL trisodium citrate solution (38.8 mmol L^{-1}) was added quickly. After the color change from pale yellow to deep red, the solution was refluxed for an additional 5 min and left to cool to room temperature. Then, the solution was diluted 5 times and stored at 4 ^{o}C for further utilized. The molar extinction coefficient (ε) around 518 nm for the AuNPs is about 2.7×10^{8} mol^{-1} cm^{-1} (Zhao et al., 2008), thus the molar concentration of the AuNPs was calculated to be nearly 1.8×10^{-9} mol L^{-1} according to Lambert Beer's law.

2.6. Parathion-methyl (PM) detection

The PM standard substance were dissolved in Tris buffer solution (10.0 mmol L^{-1}, pH=8.2) containing 10% ethanol for preparing the standard solution. Various amounts of PM standard solution were added to same TRY solution (20 ng mL^{-1}) in a 1.5 mL calibrated test tube, which were then kept in the dark for 60 min. Then, PRO (150 ng mL^{-1}) was successively added into the system. After 30 min of reaction, 0.3 mL AuNPs solution were successively added into the calibrated test tube and shaken thoroughly for 2 min. Then, 20 μL RF-QDs solution were successively added into the calibrated test tube; diluted to the mark with Tris buffer (10.0 mmol L^{-1}, pH 8.2), and shaken thoroughly for 2 min until the solution was fully mixed at room

temperature. The fluorescence spectra were recorded for PM detection.

3. Results and discussion

3.1. Characteristics of RF-QDs and AuNPs

The green emissive QDs (gQDs, curve a) and red emissive QDs (rQDs, curve b) emitted strong fluorescence with the maximal emission wavelength at 536 and 654 nm, respectively (**Fig. 1A**). Photographs of the gQDs (a) and rQDs (b) under UV illumination showed they exhibited an intense green and red fluorescence, respectively (inset of **Fig. 1A**). The RF-QDs were fabricated via hybridization of rQDs@silica microspheres and gQDs based on covalently bonding methods. The fluorescence spectrum of RF-QDs (curve c, **Fig. 1A**) showed two well-resolved emission bands under a single wavelength excitation at 380 nm, and the PL emission maximum were around 540 nm and 657 nm, respectively. When excited under UV illumination, the RF-QDs showed a strong yellow emission (inset in **Fig. 1A**), differing from that of the original gQDs and rQDs. As shown in **Fig. 1B**, the transmission electron microscopy (TEM) showed that the RF-QDs were spherical in shape and the sizes of RF-QDs were about 800 nm.

AuNPs were also characterized by UV–vis spectroscopy and TEM. **Fig. 1A** (curve d) showed the absorption spectra of AuNPs and the maximum absorption at 520 nm. It can be seen from **Fig. 1C** that the AuNPs were spherical in shape, highly monodisperse and fairly uniform with size of about 13 nm.

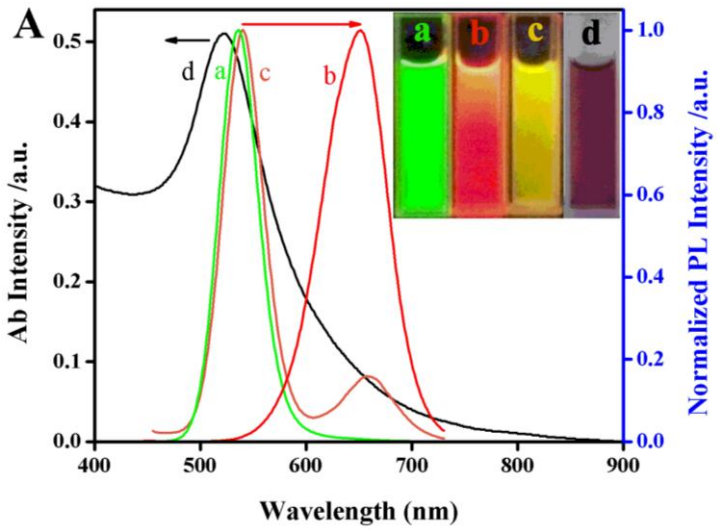

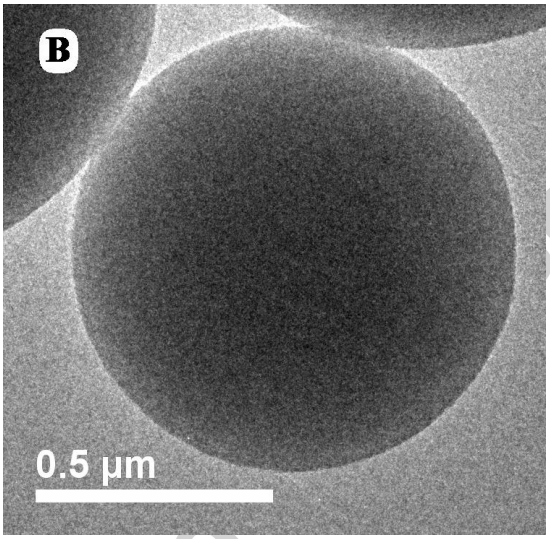

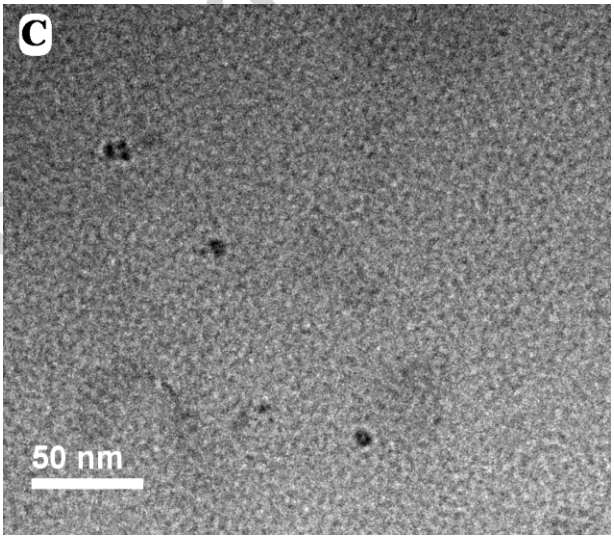

Fig. 1 (A) The fluorescence spectra of (a) QDs_{536nm}, (b) QDs_{654nm} and (c) RF-QDs, and (d) the UV-vis absorption spectrum of AuNPs. The inset shows the optical photos of (a) QDs_{536nm}, (b) QDs_{654nm} and (c) RF-QDs under UV lamp, and (d) the photos of AuNPs under sunlight. TEM

images of (B) RF-QDs and (C) AuNPs.

3.2. IFE between RF-QDs and AuNPs

The proposed biosensor consists of AuNPs and RF-QDs, where RF-QDs function as fluorometric reporter, and AuNPs serve as fluorescence quencher. According to the previous reports (Shang et al., 2009; Zhang et al., 2012; Li et al., 2013; Guo et al., 2014), the fluorescence of RF-QDs could be quenched in the presence of AuNPs through the IFE. Compared to the fluorescence resonance energy transfer-based methods, IFE does not require chemical linkage between absorber and fluorophore. There are three factors for the formation of efficient IFE. The remarkable overlap between the fluorescence emission spectrum of RF-QDs and the absorption spectrum of the AuNPs at 520 nm **(Fig. 1A)** was an indispensable factor for IFE. Furthermore, the zeta potentials of RF-QDs and AuNPs were -12.8 mV and -26.5 mV (**Fig. S1A**). Because both RF-QDs and AuNPs possess negative charges, there is no electrostatic attraction between the RF-QDs and AuNPs. Mostly important, fluorescence lifetime, which would be changed in an efficient energy transfer process, is mostly unaffected by IFE (Zhang et al., 2012). As shown in **Fig. S1B**, the fluorescence lifetime of RF-QDs was hardly changed in the presence of AuNPs. This result further suggested that the quenched fluorescence of RF-QDs was based on IFE between AuNPs and RF-QDs. To verify the existence of the IFE between AuNPs and RF-QDs, we mixed RF-QDs with different concentrations of AuNPs and monitored the fluorescence spectra of the RF-QDs. As shown in **Figure S2**, we observed a gradual decrease of PL intensity at 540 nm of the RF-QDs with the increase of the concentration of AuNPs ($0\text{-}6\times10^{-10}$ mol L^{-1}). Therefore, the PL intensity ratio (I_{540}/I_{657}) of the RF-QDs could be modulated by the absorbance of AuNPs via

IFE and 6×10^{-10} mol L^{-1} AuNPs was used in the further experiments.

3.3. Detection strategy of pesticides

As shown in **Fig. 2A**, RF-QDs exhibits a maximum fluorescent signal at 540 nm and 657 nm (curve 1), respectively. The PL intensity at 540 nm of the RF-QDs can be effectively quenched by AuNPs, while the PL intensity at 657 nm of the RF-QDs still remains unchanged with the increasing concentration of AuNPs (curve 2). So, the RF-QDs possess a built-in correction that eliminates the environmental effects and increases sensor accuracy. PRO could effectively bind to AuNPs due to the electrostatic attraction, which caused the aggregation of AuNPs and resulted in the PL intensity of RF-QDs recover (curve 3). TRY catalyzes the hydrolysis of PRO which can induce the de-aggregation of AuNPs and thus resulting in the quenching of fluorescence of RF-QDs (curve 4). When PM was added to the sensing system, the activity of TRY was inhibited and then prevented the hydrolysis of PRO. Thus, the IFE of AuNPs on RF-QDs was weakened and the PL intensity of RF-QDs was recovered again (curve 5). In order to evaluate the feasibility of this assay system for PM, the RF-QDs were individually mixed with TRY, PRO and PM, and the spectra were shown in **Fig. S3**, it can be seen that the fluorescent intensity of RF-QDs +TRY, RF-QDs+PRO and RF-QDs+PM was identical to that of RF-QDs. The TEM images of the mixture of RF-QDs and AuNPs were also recorded at different stages, which could prove the interaction among RF-QDs and AuNPs. As shown in **Fig. 2B**, AuNPs were retained in a dispersed state in the presence of RF-QDs. **Fig. 2C** showed the TEM of AuNPs in the presence of PRO and RF-QDs, indicating that no mono-dispersed AuNPs absorbed on the surface of RF-QDs. All above results indicated the sensing principle for pesticide detection is feasible.

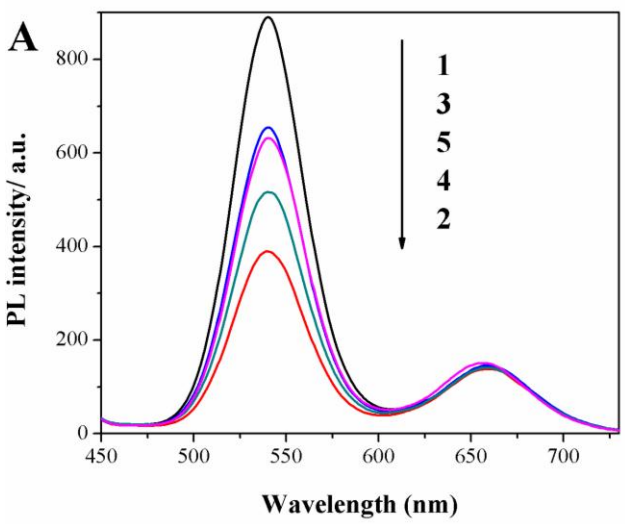

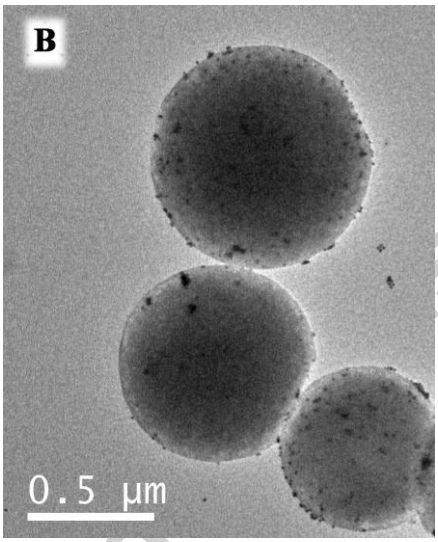

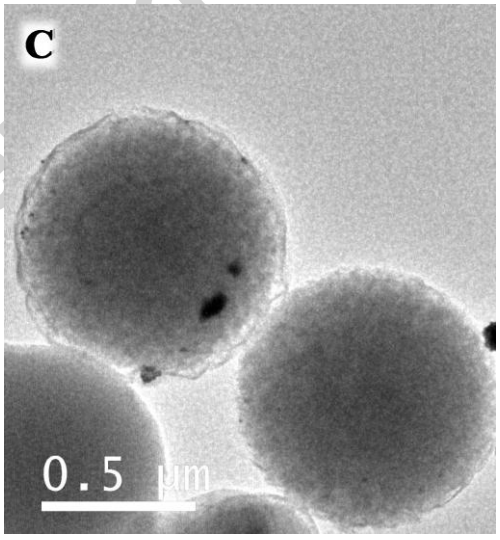

Fig. 2 (A) Fluorescence spectra of (1) RF-QDs, (2) RF-QDs and AuNPs, (3) PRO-AuNPs and RF-QDs, (4) TRY-PRO-AuNPs and RF-QDs and (5) OPs-TRY-PRO-AuNPs and RF-QDs. The final concentrations of RF-QDs, PRO, TRY, PM and AuNPs are 0.13 mg mL^{-1}, 150 ng mL^{-1}, 10 ng

mL^{-1}, 400 ng mL^{-1} and 0.6 nmol L^{-1}, respectively. TEM images of (B) the RF-QDs in the presence of AuNPs and (C) the RF-QDs in the presence of AuNPs and PRO.

3.4. The optimization

In this study, we investigated systematically the fluorescence recovery of RF-QDs induced by PRO. The fluorescence spectra of the RF-QDs in the presence of different concentration of PRO are illustrated in **Fig. S4A**. It can be seen from **Fig. S4A** that the PL intensity at 540 nm of the RF-QDs was gradually recovered with the increasing of PRO concentration in the range from 0 to 200 ng mL^{-1}, and the absorbance of AuNPs at 520 nm decreased correspondingly (**Fig. S4B)**. So 150 ng mL^{-1} PRO was used in the further experiment.

The experimental conditions for PM detection, such as reaction time, pH and reaction temperature, were also optimized in this study. The effect of reaction time on the (I_{540}/I_{657}) of the TRY-PRO-AuNPs/RF-QDs system was investigated in **Fig. S5A**. The PL intensity ratio (I_{540}/I_{657}) of the RF-QDs decreased to the minimum within 35 min and remained stable with further increase of the reaction time. So, the optimal reaction time for pesticides detection was 35 min. The effect of pH was investigated in the pH range of 6.6-9.0 (**Fig. S5B**). It can be seen that the change of PL intensity ratio of PRO-AuNPs/RF-QDs system in the presence and absence of TRY reached a maximum at pH 8.2. Therefore, pH 8.2 Tris buffer (10 mmol L^{-1}) was chosen as the optimal pH for pesticide detection. The effect of the reaction temperature on the PL intensity ratio of TRY-PRO-AuNPs/RF-QDs system was shown in **Figure S5C**. The PL intensity ratio of RF-QDs reached a minimum when the temperature reached 37 ^{o}C. Thus, 37 ^{o}C was chosen in the following experiment.

The concentrations of TRY have an influence on the hydrolysis of PRO and consequently affect the aggregation of AuNPs and the PL intensity of RF-QDs. As shown in **Fig. S6A,** with the increasing concentration of TRY, the absorbance of AuNPs at 520 nm increased rapidly, and the PL intensity at 540 nm of the RF-QDs was gradually decreased with the increase of the concentrations of TRY in the range from 0 to 1000 ng mL^{-1} (**Fig. S6B**). The linear regression equation was I_{540}/I_{657}=3.67452 − 0.27983 Log [TRY], ng mL^{-1}. The corresponding regression coefficient is 0.994. The concentration of TRY of 100 ng mL^{-1} was chosen for the pesticides detection.

3.5. Parathion-methyl detection

Fig. 3A shows the absorbance and fluorescent spectrum of TRY-PRO-AuNPs/RF-QDs system with different concentrations of parathion-methyl. As shown in **Fig. 3A,** the absorbance of AuNPs at 520 nm decreased gradually with the increasing concentration of PM. The PL intensity of the RF-QDs at 540 nm increased with the increasing of PM concentration, whereas the PL intensity around 657 nm of the embedded rQDs still remains identical (**Fig. 3B)**. The data were analyzed by the following equation (Yi et al., 2013):

$$\text{Inhibition Efficiency (IE)} = \frac{F_{\text{inhibitor}} - F_{\text{no inhibitor}}}{F_0 - F_{\text{no inhibitor}}} \times 100\%$$

Where $F_{\text{inhibitor}}$ and $F_{\text{no inhibitor}}$ refer to the PL intensity ratio of TRY-PRO-AuNPs/RF-QDs system in the presence and absence of PM, respectively. F_0 refers to the PL intensity ratio of the PRO-AuNPs/RF-QDs in the absence of TRY and PM.

A good linear relationship between the IE and the logarithm of the PM concentration was obtained in the range from 0.04 to 400 ng mL^{-1}. The regression equation is: IE (%) = 35.05 + 20.84 Log [PM], ng mL^{-1}. The corresponding regression coefficient is 0.995, and the limit of

detection (LOD) for PM is 0.018 ng L^{-1}. The maximum residue limit of PM is 100 ng mg^{-1} in rice sample set by the Ministry of Agriculture of the People's Republic of China (http://www.chinapesticide.gov.cn/mprlsv/mprls.html). Thus, our proposed methods could satisfy the detection requirements for pesticide residues in real samples. What's more, a comparison between our method and other reported methods for PM detection in linear range and LOD were summed up in **Table S1**. Compared with other sensing methods, this proposed ratiometric fluorescent methods was better than most of the reported methods.

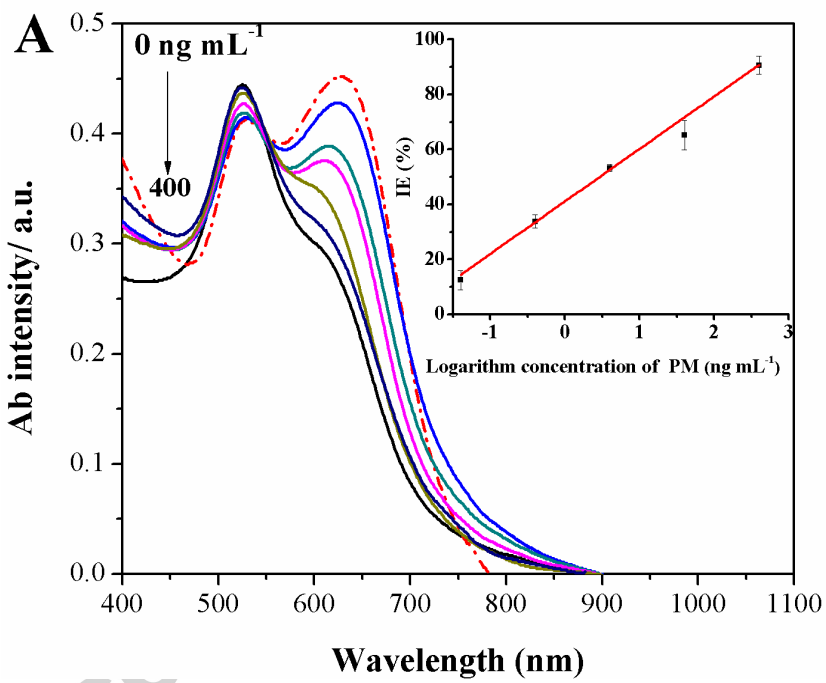

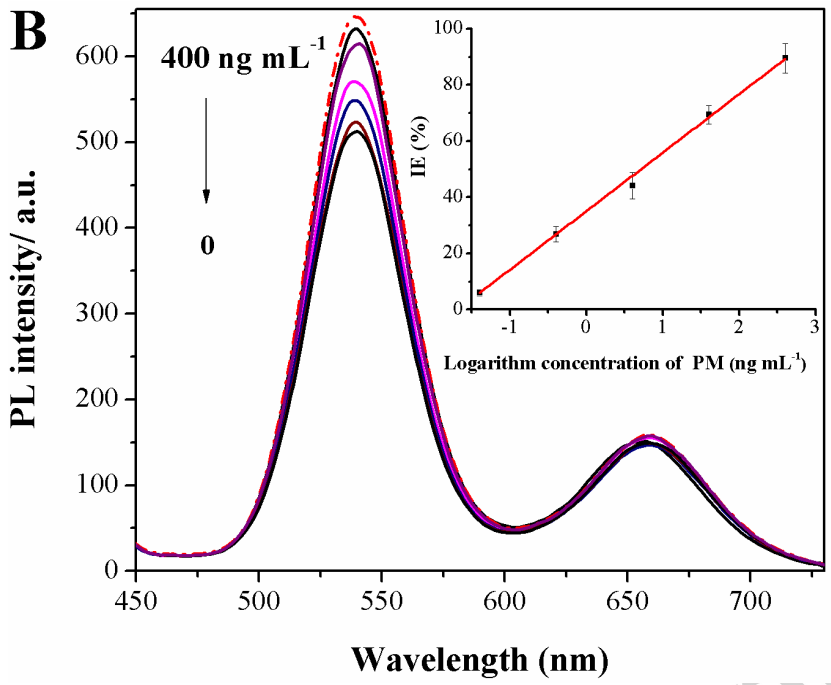

Fig. 3 (A) The absorption spectra of AuNPs upon the addition of PM at different concentrations from 0 to 400 ng mL^{-1}. (B) The fluorescence spectra of RF-QDs in the presence of different concentration of PM (0, 0.04, 0.4, 4.0, 40, 400 ng mL^{-1}). Inset: the linear plot of inhibition efficiency versus the logarithm of concentration of PM. The final concentrations of RF-QDs, PRO, TRY and AuNPs are 0.13 mg mL^{-1}, 150 ng mL^{-1}, 10 ng mL^{-1} and 0.6 nmol L^{-1}, respectively.

3.6. Selectivity for parathion-methyl detection

To evaluate the specificity of the biosensor for the detection of PM, we investigated the influences of some common existing substances in environmental and agricultural samples, including glucose, urease, horseradish peroxidase (HRP), alkaline phosphatase (ALP), lysine, histidine, threonine and tryptophan. As shown in **Fig. 4A**, after the addition of 10000 ng mL^{-1} above substance, the PL intensity ratio of PRO-AuNPs/RF-QDs system and TRY-PRO-AuNPs/RF-QDs system have no obvious change. It could be seen that the common

amine acids, proteins and enzymes do not exert evident interference on PM detection. The inhibition efficiency of the TRY-PRO-AuNPs/RF-QDs system in the presence of PM or other pesticides was shown in **Fig. 4B**. And the chemical structures of these pesticides were shown in **Fig. S7.** It can be seen that the typical carbamate pesticides, neonicotinoid insecticides and pyrethroid pesticides at the concentration of 500 ng mL^{-1} do not cause obvious interference in PM determination. And only PM and chlorpyrifos, which belongs to OPs, could cause significant inhibition efficiencies of the biosensing system. These results suggested that the established biosensors could be used for determination of different kinds of OPs. Compared with the previous biosensors based on acetylcholinesterase for pesticide detection, our proposed methods based on TRY could distinguish carbamates pesticide and OPs, indicating that this strategy had a high selectivity toward OPs.

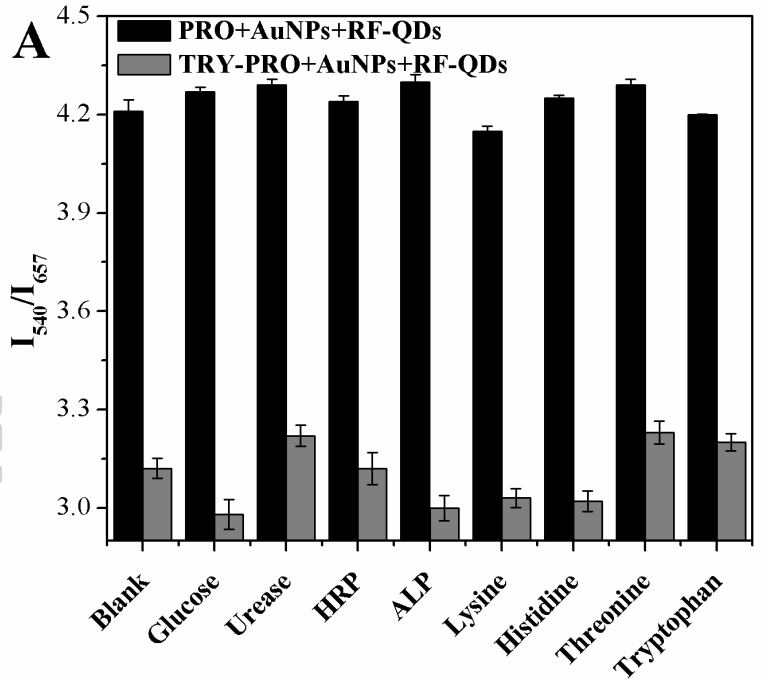

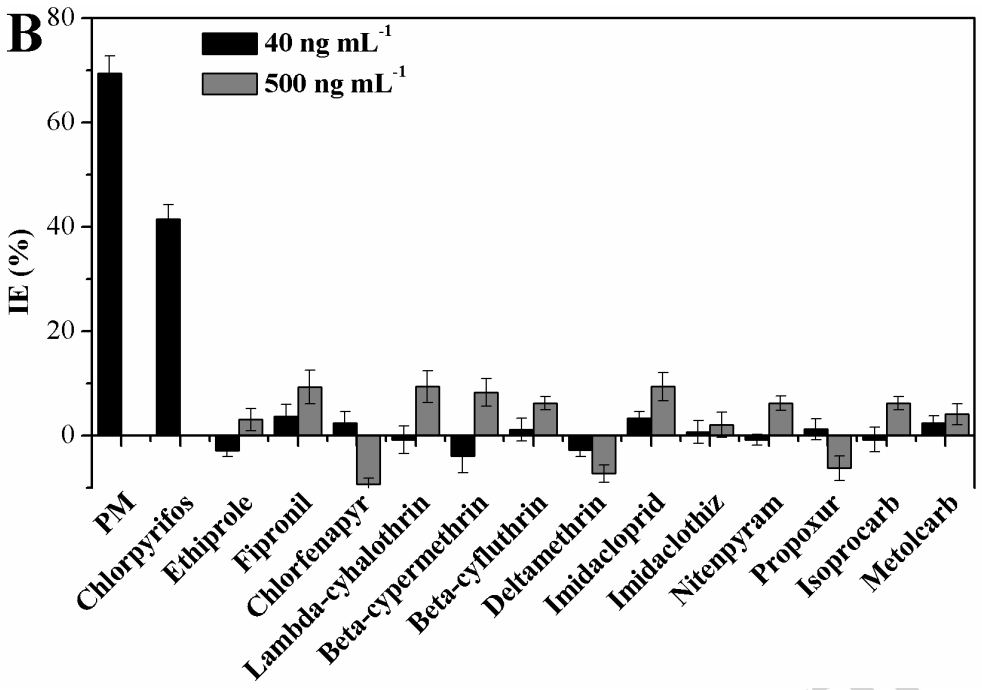

Fig. 4 (A) The PL intensity ratio of the PRO-AuNPs/RF-QDs system and TRY-PRO-AuNPs/RF-QDs system in the presence of the interfering substances (10000 ng mL^{-1}); (B) The selectivity of the ratiometric sensor to various pesticides in the Tris buffer (pH = 8.2, 10.0 mmol L^{-1}). The final concentrations of RF-QDs, PRO, TRY and AuNPs are 0.13 mg mL^{-1},150 ng mL^{-1}, 10 ng mL^{-1} and 0.6 nmol L^{-1}, respectively.

3.7. Real samples detection

In order to demonstrate the applicability of proposed sensor in real samples detection, the developed fluorescence biosensor was applied for the determination of PM in agricultural and environmental samples, such as tap water, milk and rice. The average recovery test was made by using the standard addition method, and the results were listed in **Table 1**. Moreover, comparison study of the developed biosensor with conventional method (UV spectrophotometry) for PM determination also had been carried out to confirm the performance of the developed method.

From **Table 1,** it can be seen that the results obtained by the proposed fluorescence method are in good agreement with those provided by the conventional method. The recoveries of PM in samples were between 95%-110%. The relative standard deviation (RSD) was lower than 6.33%. The results demonstrated the potential applicability of the AuNPs/RF-QD based fluorescence biosensor for the PM detection in environmental samples and agricultural products.

Table 1 Detection of PM in agricultural and environmental samples

Sample	Spiked concentration ($ng\ mL^{-1}$, $ng\ g^{-1}$)	Found PM ($ng\ mL^{-1}$ or $ng\ g^{-1}$)		Recovery (%)	RSD (n=3, %)
		UV	This methods		
Tap water	0.2	/	0.19	95.00	2.74
	4	/	4.17	104.25	3.55
	200	199.19	202.36	101.59	2.69
Milk	0.2	/	0.22	110.00	5.72
	4	/	4.34	108.50	5.08
	200	201.34	207.76	103.88	6.33
Rice	0.2	/	1.9	95.00	5.20
	4	/	3.85	96.25	4.64
	200	197.36	196.35	98.18	4.75

4. Conclusions

In summary, we have developed a novel sensor for organophosphorus pesticides detection based on the IFE between the RF-QDs and AuNPs. RF-QDs which constructed by hybridization of two differently colored quantum dots, possess a built-in correction that eliminates the environmental effects and increases sensor accuracy. This biosensor has many advantages, such as highly sensitivity, a wide linear range and high selectivity. The proposed method was successfully applied to the determination of PM in agricultural samples with satisfactory results and good repeatability.

Acknowledgements

This work was financially supported by the National Natural Science Foundation of China (Nos. 21075050, No. 21275063) and the Science and Technology Development Project of Jilin Province,

China (No. 20110334).

References

Chen, L.X., Fu, X.L., Li, J.H., 2013. Nanoscale 4, 5905–5911.

Chen, T.T., Hu, Y.H., Cen, Y., Chu, X., Lu, Y., 2013. J. Am. Chem. Soc. 135, 11595–11602.

Du, D., Wang, J., Wang, L.M., Lu, D.L., Lin, Y.H., 2011. Anal. Chem. 84, 1380–1385.

Gao, X., Tang, G.C., Su, X.G., 2012. Biosens. Bioelectron. 36, 75–80.

Grabar, K.C., Brown, K.R., Keating, C.D., Stranick, S.J., Tang, S.L., Natan, M.J., 1997. Anal. Chem. 69, 471–477.

Guo, J.J., Liu, X., Gao, H.T., Bie, J.X., Zhang, Y., Liu B.F., Sun, C.Y., 2014. RSC Adv. 4, 27228–27235.

Huang, G.M., Ouyang, J., Baeyens, W.R., Yang, Y.P., Tao, C.J., 2002. Anal. Chim. Acta 474, 21–29.

Hou, J.Y., Dong, J., Zhu, H.S., Teng, X., Ai, S.Y., Mang, M.L., 2015. Biosens. Bioelectron. 68, 20–26.

Jena, B.K., Retna Raj, C., 2008. Biosens. Bioelectron. 23, 1285–1290.

Jha, N., Ramaprabhu, S., 2010. Nanoscale 2, 806–810.

Li, J.W., Li, X.M., Shi, X.J., He, X.W., Wei, W., Ma, N., Chen, H., 2013. ACS Appl. Mater. Interfaces 5, 9798–9802.

Liu, D.B., Chen, W.W., Wei, J.H., Li, X.B., Wang, Z., Jiang, X.Y., 2012. Anal. Chem. 84, 4185–4191.

Liu, G.Z., Guo, W.Q., Yin, Z., 2014. Biosens. Bioelectron. 53, 440–446.

Long, Q., Li, H.T., Zhang, Y.Y., Yao, S.Z., 2015. Biosens. Bioelectron. 68, 168–174.

Meng, X.W., Wei, J.F., Ren, X.L., Ren, J., Tang, F.Q., 2013. Biosens. Bioelectron. 47, 402–407.

Quistad, G. B., Casida, J. E., 2000. J. Biochem. Mol. Toxicol. 14, 51–56.

Ruark, C.D., Eric Hack, C., Robinson, P.J., Gearhart, J.M., 2011. J. Toxicol. Environ. Health A 74, 1–23.

Shang, L., Dong, S.J., 2009. Anal. Chem. 81, 1465–1467.

Tyrakowski, C.M., Snee, P.T., 2014. Anal. Chem. 86, 2380–2386.

Wang, K., Qian, J., Jiang, D., Yang, Z.T., Du, X.J., Wang, K., 2015. Biosens. Bioelectron. 65, 83–90.

Wang, C., Ma, Q., Su, X.G., 2008. J. Nanosci. Nanotechno. 8, 4408–4414.

Wu, C.F., Chiu, D.T., 2013. Angew. Chem. Int. Ed. 52, 3086–3109.

Wu, J.C., Zou,Y., Li, C.Y., Sicking, W., Piantanida, I., Yi, T., Schmuck, C., 2012. J. Am. Chem. Soc. 134, 1958–1961.

Yao, J.L., Zhang, K., Zhu, H.J., Ma, F., Sun, M.T., Yu, H., Sun, J., Wang, S.H., 2013. Anal. Chem. 85, 6461–6468.

Yan, X., Li, H.X., Li, Y., Su, X.G., 2014a. Anal. Chim. Acta 852, 189–195.

Yan, X., Li, H.X., Wang, X.Y., Su, X.G., 2015a. Talanta 131, 88–94.

Yan, X., Li, H.X., Yan, Y., Su, X.G., 2015b. Food Chem. 173, 179–184.

Yan, X., Li, H.X., Yan, Y., Su, X.G., 2014b. Anal. Methods 6, 3543–3554.

Yi, Y.H., Zhu, G.B., Liu, C., Huang, Y., Zhang, Y.Y., Li, H.T., Zhao, J.N., Yao, S.Z., 2013. Anal. Chem. 85, 11464–11470.

Zacharis, C.K., Christophoridis, C., Fytianos, K., 2012. J. Sep. Sci. 35, 2422–2429.

Zong, C.H., Ai, K., Zhang, G., Li, H.W., Lu, L.H., 2011. Anal. Chem. 83, 3126–3132.

Zhang, L., Zhang, A.D., Du, D., Lin, Y.H., 2012. Nanoscale 4, 4674–4679.

Zhang, M.W., Cao, X.Y., Li, H.K., Guan, F.R., Guo, J.J., Shen, F., Luo, Y.L., Sun, C.Y., Zhang, L.G., 2012. Food Chem. 35, 1894–1900.

Zhang, K., Mei, Q.S., Guan, G.J., Liu, B.H., Wang, S.H., Zhang, Z.P., 2010. Anal. Chem. 82, 9579–9586.

Zhang, K., Zhou, H.B., Mei, Q.S., Wang, S.H., Guan, G.J., Liu, R.Y., Zhang, J., Zhang, Z.P., 2011. J. Am. Chem. Soc. 133, 8424–8427.

Zhao, X.S., Kong, W.J., Wei, J.H., Yang, M.H., 2014. Food chem. 162, 270-276. Zhao, W.A., Brook, M.A., Li, Y.F., 2008. Chem. Bio. Chem. 9, 2363–2371.

Zheng, Z.Z., Li, X.Y., Dai, Z.F., Liu, S.Q., Tang, Z.Y., 2011a. J. Mater. Chem. 21, 16955–16962.

Zheng, Z.Z., Zhou, Y., Li, X., Liu, S.Q., Tang, Z.Y., 2011b. Biosens. Bioelectron. 26, 3081–3085.

Zhou, C.B., Li, W.Y., Chen, J., Yang, M.D., Li, Y., Zhu, J.T., Yu, C., 2014. Analyst 139, 1057–1062.

Highlights:

►The ratiometric fluorescent QDs which was fabricated by two different QDs, possess a built-in correction that eliminates false signals.

► The fluorescence intensity of ratiometric fluorescent QDs could be quenched by AuNPs based on inner-filter effect.

►The proposed approach for parathion-methyl detection has a much lower LOD down to 0.018 $ng \cdot mL^{-1}$.

► Parathion-methyl in real sample was detected with satisfactory results.